Laser mediated cartilage reshaping

Wong, B.J.F.

Publication date
2001

Lasers in Surgery and Medicine 27:119–128 (2000)

Optical and Thermal Properties of Nasal Septal Cartilage

Jong-In Youn, MS,[1]* Sergey A. Telenkov, PhD,[1] Eunha Kim, MS,[1] Naresh C. Bhavaraju, MS,[1] B.J.F. Wong, MD,[2] Jonathan W. Valvano, PhD,[1] and Thomas E. Milner, PhD[1]

[1]Biomedical Engineering Program, University of Texas at Austin, Austin, Texas
[2]Beckman Laser Institute and Medical Clinic, University of California Irvine, Irvine, California

Backgrounds and Objectives: **The aim of the study was to measure the spectral dependence of optical absorption and reduced scattering coefficients and thermal conductivity and diffusivity of porcine nasal septal cartilage. Values of optical and thermal properties determined in this study may aid in determining laser dosimetry and allow selection of an optical source wavelength for noninvasive diagnostics for laser-assisted reshaping of cartilage.**
Materials and Methods: **The diffuse reflectance and transmittance of ex vivo porcine nasal septal cartilage were measured in the 400- to 1,400-nm spectral range by using a spectrophotometer. The reflectance and transmittance data were analyzed by using an inverse adding-doubling algorithm to obtain the absorption (μ_a) and reduced scattering (μ_a') coefficients. A multichannel thermal probe controller system and infrared imaging radiometer methods were applied to measure the thermal properties of cartilage. The multichannel thermal probe controller system was used as an invasive technique to measure thermal conductivity and diffusivity of cartilage at three temperatures (27, 37, 50°C). An infrared imaging radiometer was used as a noninvasive method to measure the thermal diffusivity of cartilage by using a CO_2 laser source (λ = 10.6 μm) and an infrared focal plane array (IR-FPA) camera.**
Results: **The optical absorption peaks at 980 nm and 1,180 nm in cartilage were observed and corresponded to known absorption bands of water. The determined reduced scattering coefficient gradually decreased at longer wavelengths. The thermal conductivity values of cartilage measured by using an invasive probe at 27, 37, and 50°C were 4.78, 5.18, and 5.76 mW/cm°C, respectively. The corresponding thermal diffusivity values were 1.28, 1.31, and 1.40× 10^{-3} cm^2/sec. Because no statistically significant difference in thermal diffusivity values with increasing temperature is found, the average thermal diffusivity is 1.32 × 10^{-3} cm^2/sec. The numerical estimate for thermal diffusivity obtained from infrared radiometry measurements was 1.38 × 10^{-3} cm^2/sec.**
Conclusion: **Values of the spectral dependence of the optical absorption and reduced scattering coefficients, and thermal conductivity and diffusivity of cartilage were measured. The invasive and noninvasive diffusivity measurements were consistent and concluded that the infrared imaging radiometric technique has an advantage to determine thermal properties, because damage to the cartilage sample may be**

Contract grant sponsor: Whitaker Foundation; Contract grant sponsor: National Institute of Health; Contract grant sponsor: The University of Texas Faculty Development Program, New Star Lasers Inc.

*Correspondence to: Jong-In Youn, MS, Biomedical Engineering Program, University of Texas at Austin, Austin, TX 78712. E-mail: yji97@mail.utexas.edu

Accepted 13 March 2000

avoided. The measured values of absorption and reduced scattering coefficients can be used for predicting the optical fluence distribution in cartilage and determining optical source wavelengths for the laser-assisted cartilage reshaping studies. The thermal conductivity and diffusivity values can play role in understanding thermal-dependent phenomenon in cartilage during laser irradiation and determining laser dosimetry for the laser-assisted cartilage reshaping studies. Lasers Surg. Med. 27:119–128, 2000. © 2000 Wiley-Liss, Inc.

Key words: laser-assisted cartilage reshaping; diffuse reflectance; transmittance; absorption coefficient; reduced scattering coefficient; thermal conductivity; thermal diffusivity

INTRODUCTION

With progressive use of lasers in medical applications, an increasing need is recognized to study the optical properties and heat-transfer mechanisms in biological tissue. Understanding propagation of laser light in tissue begins with knowledge of the photobiological effects as well as spatial distribution of optical fluence [1]. Knowledge of the optical and thermal properties of cartilage may aid for diagnostics and laser dosimetry determination in laser-assisted cartilage reshaping studies [2–10]. Many investigators have reported studies describing the laser modification of cartilage, especially articular cartilage, by using different light sources such as XeCl eximer laser (λ = 308 nm) [11], KrF eximer laser (λ = 248 nm) [12], Nd:YAG laser (λ = 1.064 μm) [13], and Ho:YAG laser (λ = 2.1 μm) [14].

In laser-assisted cartilage reshaping, first introduced by Sobol by using CO_2 laser (λ = 10. μm) in the ear and nose of rabbits and human cartilage in 1993, light scattering has been used to identify the phase transformation in cartilage after laser irradiation [15]. Sobol presented that under the effect of laser irradiation, mechanically deformed cartilage undergoes a temperature-dependent phase transformation, resulting in accelerated stress relaxation and hypothesized that cartilage can be affected by the distribution of internal stresses from local laser heating and, thus, reshape without ablation [15]. In a later study of laser-assisted cartilage reshaping, Sobol et al. measured temperature and stress in cartilage under Holmium laser irradiation and argued that the reshaping of cartilage is connected with the bound-to-free transformation of water at a temperature around 70°C [6–10]. On the other hand, Wong et al. investigated integrated backscattered light intensity of He:Ne laser light (λ = 632.8 nm) and radiometric surface temperature changes of cartilage during laser irradiation by using a Nd:YAG laser (λ = 1.32 μm) [3–5]. Wong et al. presented that internal stress relaxation of cartilage occurred approximately 65°C and integrated backscattered light intensity were observed to increase, plateau, and then decrease [3–5].

Notwithstanding the importance of the optical properties of cartilage, limited studies have been reported providing absorption and scattering coefficient data. Ebert et al. investigated optical properties of weight-bearing and nonweight-bearing equine articular cartilage in the 300–850 nm spectral range [16]. Although they found no statistical differences in scattering coefficients between the weight-bearing and non–weight-bearing cartilage, stronger absorption in weight-bearing compared with non–weight-bearing cartilage was reported [16]. Although most cartilage in the body is composed of similar chemical structures such as water, collagen, and proteoglycans, these constituents are present in different proportions [17–19]. Because of the varying composition, the optical properties of nasal septal cartilage are distinct from those of articular cartilage. Knowledge of optical properties of cartilage may be important for development of noninvasive optical diagnostics to minimize nonspecific thermal damage in laser-assisted cartilage reshaping procedures.

Knowledge of thermal properties of biological tissue is useful for understanding and predicting the results of therapeutic and diagnostic procedures. Two important thermal properties relevant to laser surgical procedures are thermal conductivity (K) and diffusivity (α) [1,20]. Therefore, measurement of K and α is necessary to specify laser dosimetry in laser-assisted cartilage reshaping.

For the thermal property measurements of cartilage, two methods that used a multichannel thermal probe controller system and infrared imaging radiometry were applied. For invasive stud-

ies, a thermal measurement technique originally introduced by Chato [21] simultaneously uses thermistor probes as a heat source and a temperature sensor. This technique has been improved by many investigators and been applied to measure thermal properties of various biological materials such as heart, kidney, liver, arterial wall, and atherosclerotic plaque [1,22,23]. Inasmuch as the invasive procedures generally use a glass-encapsulated spherical thermistor, insertion of the thermistor into soft tissues is convenient by using a hypodermic needle [21] or plastic catheter [24]. Alternatively, for measurement of hard tissues, limited investigations have been performed probably because of the technical challenge to insert a thermal probe within hard tissue without damaging the probe while maintaining good thermal contact [25]. In this study, by using a personal computer based multichannel thermal-probe controller system developed by Valvano et al. [1,22,23,26], thermal conductivity and diffusivity of porcine nasal septal cartilage were measured at three temperatures (27, 37, 50°C).

For noninvasive studies, Milner et al. [27] introduced a noncontact method to determine the thermal diffusivity of biological materials by using a laser source and an infrared focal plane array (IR-FPA) camera. The method is based on estimates of the lateral thermal point spread function by using as input data pairs of infrared emission images recorded after pulsed laser irradiation. Thermal diffusivity of test specimens is determined from the best fit to the lateral thermal point spread function determined from many recorded image pairs [27].

Laser irradiation of cartilage under mechanical deformation may be used for permanent reshaping without causing ablation. Although knowledge of the cartilage reshaping mechanisms under laser irradiation is incompletely understood, the absorption and reduced scattering coefficient values may aid in selection of optical source wavelengths for diagnostic instrumentation to identify the phase transition. In addition, measurements of thermal conductivity and diffusivity may be helpful to determine laser dosimetry for laser-assisted cartilage reshaping.

MATERIALS AND METHODS

Nasal Septal Cartilage Harvest

The nasal septal cartilage extraction procedure was approved by Animal Resource Center of The University of Texas at Austin (Protocol 99020101). Before the experiment, a fresh porcine head was obtained from a local abattoir. The prepared porcine head was placed on an operating table and explored for an incision line. The skin was removed from the upper side of the head through the bilateral nasal side. By using a standard carpenter's hammer and chisel, bilateral nasal bone osteotomies were performed along the line of incision. The hard bone was removed from the site, being careful not to damage the sample material, and the nasal cartilage specimen was removed by using a chisel. After extraction, soft tissue including perichondrium was peeled away from the cartilage specimen and the sample was rinsed in tap water for approximately 15 minutes to remove hemocytes. The sample was stored in physiological saline at 4°C for experimental use.

Optical Absorption and Scattering Measurements

By using a scalpel, the cartilage specimens were sliced in rectangular parallelepiped shapes ($23 \times 23 \times 1.5$ mm^3) and placed between two glass microscope slides to prevent dehydration and to maintain a flat surface. The thickness of the slide-sample-slide assembly was measured with a micrometer, and the actual sample thickness was obtained by subtracting the combined thickness of the microscope slides.

A Varian Cary 4E Spectrophotometer with a diffuse reflectance accessory was used to measure reflectance and transmittance of the samples. After baseline calibration of the spectrophotometer, the prepared sample assembly was placed onto the sample port of the integrating sphere to record reflectance. After the reflectance measurement, the assembly was detached and the baseline correction was performed again. The sample assembly was then mounted on the entrance port of the integrating sphere to measure the transmittance. Reflectance and transmittance data were recorded from 400 to 2,500 nm at 1-nm intervals. After the spectrophotometric measurement, an inverse-adding doubling computer program written by Scott Prahl [1] was used to obtain absorption and reduced scattering coefficients by using, as input, reflectance and transmittance data. The value of sample refractive index (n) was required as input data for the computer program. Because few measurements of the refractive index of cartilage have been reported, the value of n used was taken from the data reported by Wang et al. with hydrated type I collagen samples by using optical low-coherence reflectometry at λ =

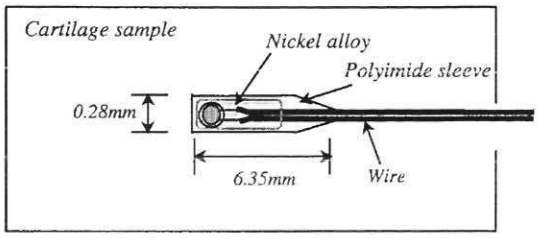

Fig. 1. Thermal probe assembly to measure thermal conductivity and diffusivity [29].

850 nm [28]. Wang et al. measured the refractive index of hydrated type I collagen films, because the optical properties are similar to those of human connective tissue [28]. Wang et al. gave the average value for the group refractive index of dry and fully hydrated collagen films at $\lambda = 850$ nm and $n = 1.53 \pm 0.02$ and 1.43 ± 0.02, respectively [28]. For refractive index of cartilage, $n = 1.43$ was used for the input parameter to the inverse adding-doubling computer program in this experiment.

Thermal Conductivity and Diffusivity Measurements

Invasive probe for thermal conductivity and diffusivity measurement. The nasal septal cartilage samples were cut into rectangular parallelepiped shapes approximately 7.6 × 20 mm^2 (width × length). The thickness of the cartilage samples was approximately 5 mm and varied with each animal. Thermal properties of cartilage samples were measured within 2 hours after time of animal killing.

To measure thermal properties of nasal septal cartilage, a small thermal probe assembly (AB6E8 with BR11KA102J thermistor; diameter, 0.28 mm; length, 6.35 mm) manufactured by Thermometrics (Edison, NJ) was used (Fig. 1). The relatively small thermal probe was used to speed the time response of the measurement, reduce invasiveness, and reduce the measurement volume so that the probe did not extend beyond the boundaries of the cartilage sample surface [1,22,23]. Because the description of the theoretical model and numerical algorithm used for computation of thermal conductivity and diffusivity is presented by Valvano et al. [1,22–24], we will not report the details of the theory of operation.

In our study, a 20-gauge (outer diameter, D = 0.91 mm) hypodermic needle was inserted into the side of the cartilage sample until the tip of the needle was at a depth of approximately 15 mm. The needle was then withdrawn, and the probe was inserted into the cavity as far as possible to minimize the gap between the bottom of the hole and tip of the thermal probe. This placement allowed the thermal probe to remain completely imbedded in the cartilage sample during measurement. The sample-probe assembly was then wrapped in a plastic sheet to prevent water contact with the cartilage sample surface and immersed in a constant temperature bath. After initialization of the multichannel controller system, the thermistors were initialized and electrical power was delivered to the thermistors. Measurements of electrical power and temperature difference between the heated thermistors and the baseline tissue were used to calculate the thermal conductivity and diffusivity of the cartilage sample [1,22,23].

Noninvasive technique for thermal diffusivity measurement. Recent studies by Milner et al. [27] demonstrated that principles of infrared imaging radiometry can be used for noncontact measurement of thermal diffusivity in biological materials. The noninvasive nature of infrared imaging radiometry provides an alternative approach to invasive probes for measurement of cartilage thermal diffusivity. Because description of the theoretical model and numerical algorithm used for computation of thermal diffusivity is presented by Milner et al. [27], we will not report the details of the technique and will describe only essential features.

When heat diffuses in the sample and two successive image frames are recorded, the later frame can be written as a convolution of the first frame with a lateral thermal point spread function. The lateral thermal point spread function is characterized by thermal diffusivity of the sample. We applied this technique for noninvasive measurements of thermal diffusivity of cartilage. Thermal diffusivity is estimated by finding a parametric fit to the lateral thermal point spread function.

Focused radiation emitted by a CO_2 laser ($\lambda = 10.6$ μm, Model 1055, Sharplan Lasers, Inc.) with a pulse duration of 100 μsec and average output power of 0.1 W was used for localized heating of a fresh cartilage specimen (Fig. 2) maintained at room temperature (27°C). Strongly absorbed CO_2 laser radiation was focused to a spot with a 0.6-mm diameter to give a spatially local-

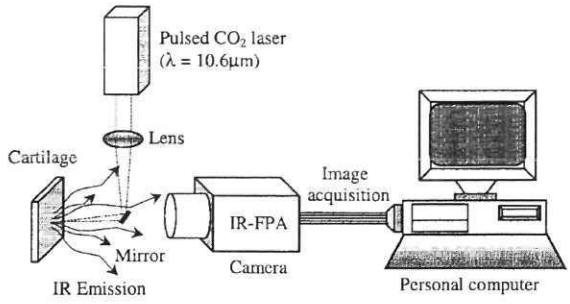

Fig. 2. Schematic diagram of noninvasive measurement of thermal diffusivity in cartilage by infrared imaging radiometry technique.

ized temperature peak on the cartilage surface. Digital infrared emission images were recorded immediately after pulsed laser exposure by an InSb focal plane array camera (Amber Engineering, Goleta, CA, 3–5 μm, 256 × 256 pixels) at frame rate of 60 Hz. Pairs of IR emission images recorded 0.1 second apart were used to evaluate the lateral thermal point spread function and, hence, thermal diffusivity. The selected time interval between the two image frames used in our computation allowed sufficient lateral heat diffusion while maintaining signal-to-noise ratio in both images. A total of five image sequences acquired for two different cartilage samples were used to determine thermal diffusivity.

RESULTS

Transmittance and Reflectance

Measured transmittance and reflectance spectra of a porcine nasal septal cartilage sample over the 400–1,400 nm spectral range are presented in Figure 3. As observed in Figure 3A, transmittance spectra exhibit absorption features corresponding to hemoglobin near 577 and 540 nm and water at ~980 nm and 1,180 nm. The reflectance curve steadily decreases with increasing wavelength in the 400–1,400 nm spectral range (Fig. 3B).

Absorption and Reduced Scattering Coefficients

To determine absorption and reduced scattering coefficients of cartilage by using the reflection and transmission data, the inverse adding-doubling method was applied [30]. Averaged spectra for the absorption (μ_a) and reduced scattering coefficients (μ_s') obtained from 25 cartilage samples are presented in Figure 4. Peak values in μ_a at 980 and 1,180 nm correspond to known absorption bands of water [31,32]. The reduced scattering coefficient (Fig. 4B) steadily decreases with increasing wavelength. The measured absorption coefficients of cartilage (μ_{ac}) were compared with known values of water (μ_{aw}) [31,32]. The ratio, $\mu_{ac}(\lambda)/\mu_{aw}(\lambda)$ at λ = 1,150 nm is 0.7 and is consistent with known fractional water concentration of cartilage (0.65–0.85) [15]. At wavelengths (e.g., λ = ~980 nm) where water absorption is peaked, μ_{ac} gives too large a fractional water concentration (~0.9–1.0). When the uncertainty in μ_{ac} is considered, however, values are consistent with the known fractional water concentration.

The optical properties of cartilage were measured after laser irradiation. Light emitted from a Nd:YAG laser (λ = 1.32 μm, 6 W, frequency = 10 Hz, t_p ~700 μsec, model 130, New Star Lasers, Inc.) was applied to heat the cartilage sample for ~6 seconds and a spot size of 5 mm in diameter. Cartilage sample thickness (t = 1.613 mm) decreased by approximately 5.8% after laser irradiation. The absorption and reduced scattering coefficients of cartilage were slightly lower than those of nonirradiated control samples at λ = 630 nm. At λ = 1,320 nm, the absorption and reduced scattering coefficients were slightly higher than that of nonirradiated control samples. These changes may be caused by dehydration, change in thickness, or denaturation of irradiated cartilage due to laser heating.

An experiment was performed to compare the optical properties of nasal septal and aural cartilage. As seen in Figure 5, aural cartilage absorbs two times more strongly than nasal septal cartilage in the near infrared region. The reduced scattering coefficients of aural cartilage (two samples) are substantially higher than that of nasal septal cartilage. The result indicates the possibly different physiologic structure and/or relative composition of molecular constituents between aural and nasal septal cartilage.

Thermal Conductivity and Diffusivity Measurements

For the invasive probe measurement, thermal conductivity and diffusivity were measured at three different temperatures (27, 37, 50°C). Table 1 shows the thermal conductivity and diffusivity values. These values were obtained by using 15 fresh samples, and the measurement was performed 11–15 times at each temperature.

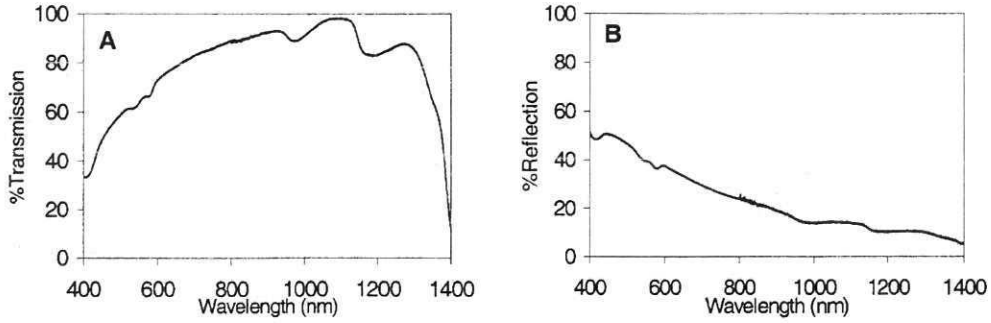

Fig. 3. Transmittance (**A**) and reflectance (**B**) spectra of a porcine nasal septal cartilage sample in the 400- to 1,400-nm spectral region. Sample thickness = 1.36 mm.

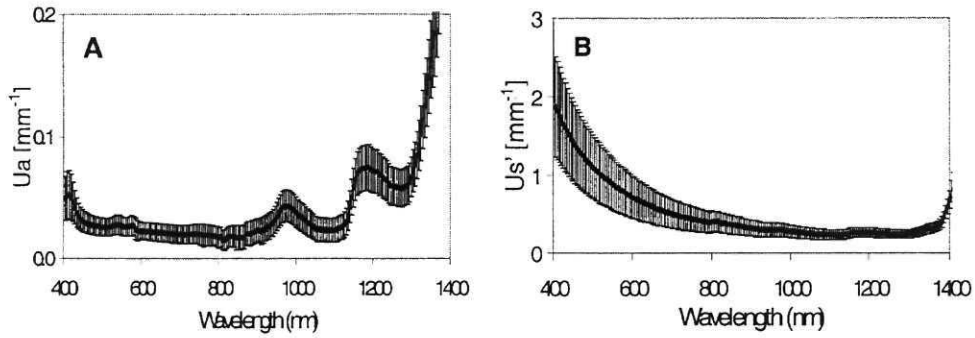

Fig. 4. Average absorption (**A**) and reduced scattering (**B**) coefficients of cartilage in the 400- to 1,400-nm spectral region captured by using inverse adding-doubling algorithm with 25 cartilage samples (n = 1.43).

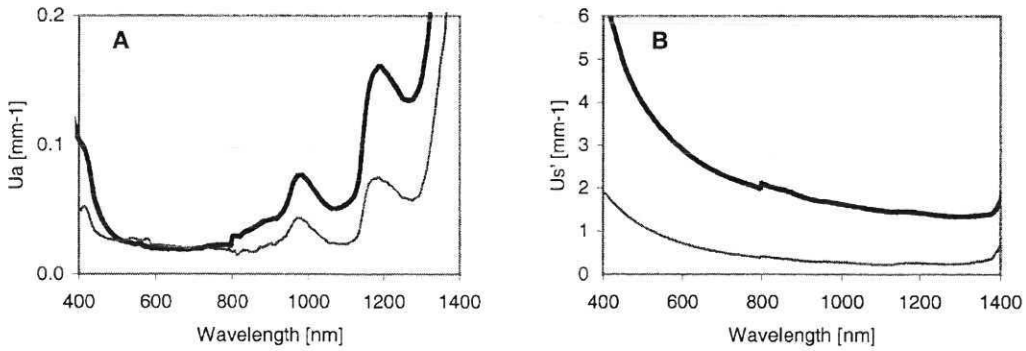

Fig. 5. Absorption (**A**) and reduced scattering (**B**) coefficients of aural (thick line) and nasal septal (thin line) cartilage samples.

Thermal conductivity and diffusivity values increased with increasing temperature.

A t-test was used to check whether the difference between values obtained at different temperatures is statistically significant [33].

$$t = \frac{\bar{x}_1 - \bar{x}_2}{\sqrt{\frac{s_1^2}{n_1} + \frac{s_2^2}{n_2}}}$$

Here t is a t-distribution critical value, $\underline{x}_1$ and $\underline{x}_2$ are sample means, s_1 and s_2 are sample standard deviations, and n_1 and n_2 are sample sizes. On the basis of the results of the t-test, thermal conductivity values gave greater than 90% confidence that a statistically significant difference exists with increasing temperature. No statistically significant difference in thermal diffusivity values with increasing temperature was found.

TABLE 1. Thermal Conductivity and Diffusivity of Porcine Nasal Septal Cartilage at 27, 37, and 50°C Using Thermal Probe Assembly*

	Temperature		
Thermal properties	27°C	37°C	50°C
Conductivity (mW/cm°C)	4.783 ± 0.825 (15)	5.182 ± 0.291 (14)	5.757 ± 0.502 (11)
Diffusivity ($\times 10^3$ cm^2/s)	1.284 ± 0.294 (15)	1.310 ± 0.163 (14)	1.397 ± 0.202 (11)

*The values in parentheses are sample numbers, and the sample thickness is from 3 mm to 5 mm.

For the noninvasive measurements of thermal diffusivity by using infrared imaging radiometry, our numerical algorithm displayed fast convergence and gave an estimate for thermal diffusivity of cartilage $D = 1.38 \pm 0.26 \times 10^{-3}$ cm^2/sec at T = 27°C. This value was consistent with that of the invasive measurement by using the multichannel thermal probe controller system (see Table 1).

DISCUSSION AND CONCLUSION

The principal advantages of using laser irradiation for the generation of thermal energy in tissue are precise control of both the space-time temperature distribution and time-dependent thermal denaturation kinetics. During laser irradiation, mechanically deformed cartilage tissue undergoes a temperature dependent phase transformation resulting in accelerated stress relaxation without causing ablation [15]. When a critical temperature is attained, cartilage becomes plastic and may be molded into new shapes that harden as the tissue cools [3]. Clinically, this reshaped cartilage tissue can be used to recreate the underlying cartilaginous framework of structures in the head and neck such as ear, larynx, trachea, and nose [2–5,15]. Therefore, optimization of the laser-assisted cartilage reshaping process requires identification of the optical and temperature dependence of the phase transformation and its relationship to observed changes in cartilage optical and thermal properties.

The spectroscopic analysis and inverse adding doubling algorithm for optical property measurement in biological tissue are completed to develop models describing light propagation in many mammalian tissues [11–14,16]. Concerning cartilage, most studies of the optical properties have been reported involving articular cartilage because of the increasing use of lasers in joint surgery. Ebert et al. measured the absolute total reflectance of weight-bearing and nonweight-bearing equine articular cartilage in the 300- to 850-nm spectral range by using a spectrometer with an attached integrating sphere [16]. These authors included Kubelka-Munk absorption and scattering coefficients, light density distributions, and light penetration depth [16]. Because Kubelka-Munk absorption and scattering coefficients cannot be directly compared with our measured absorption and reduced scattering coefficients, an approximation relating Kubelka-Munk and transport theory parameters by Klier [34] and van Gemert and Star [35] was applied. The Kublka-Munk absorption (A_{km}) and scattering coefficients (S_{km}) are related to transport values by $A_{km} \cong 2\mu_a$ and $S_{km} \cong \frac{3}{4}\ \mu_s'$ [34,35]. From the results of optical properties from articular cartilage in the 400- to 850-nm spectral region, the absorption coefficients were up to 2.5-fold higher than the values of nasal septal cartilage found in our study. For the reduced scattering coefficients, the values of articular cartilage were also up to two-fold higher than those of nasal septal cartilage reported here. The results indicate that articular cartilage may absorb and scatter light more strongly than nasal septal cartilage over the 400- to 850-nm spectral region.

Raunest and Schwarzmaier also measured optical density of articular cartilage by microspectroscopy in the 250- to 750-nm spectral range to examine the potential for selective laser irradiation [36]. These authors presented a more narrow spectral range than Ebert et al. and did not include calculation of absorption or scattering coefficients [36]. In contrast, nasal septal cartilage with different constituents and molecular structure from articular cartilage has been modified by using longer wavelength laser sources. With respect to laser-assisted reshaping of nasal septal cartilage, various sources such as He:Ne laser (λ = 632.8 nm) for investigating light scattering properties and Nd:YAG laser (λ = 1.32 μm) or CO_2 laser (λ = 10.6 μm) for the heating source were used to identify the phase transformation during laser irradiation [2–5,15]. Therefore, the spectral region that is needed to study laser-assisted reshaping of nasal septal cartilage is broader than what has been reported. Values of

TABLE 2. Absorption and Reduced Scattering Coefficients of Cartilage at 630 nm and 1320 nm*

Sample numbers	Sample thickness (mm)	Wavelength (nm) 630 μ_a (mm^{-1})	630 μ_s' (mm^{-1})	1,320 μ_a (mm^{-1})	1,320 μ_s' (mm^{-1})
25	1.466 (0.374)	0.022 (0.006)	0.559 (0.127)	0.095 (0.015)	0.237 (0.037)

*The values in parentheses are standard deviations.

optical and thermal properties determined in this study allow selection of an optical source wavelength for noninvasive optical diagnostics and aid in determining laser dosimetry for the laser-assisted cartilage reshaping studies.

In Table 2, the absorption coefficient (μ_a) and reduced scattering coefficient (μ_s') of nasal septal cartilage are compared at 630 nm and 1,320 nm. The data in Table 2 were compared with values from the literature. Beek et al. [37] reported the absorption and reduced scattering coefficient of rabbit cartilage at 632.8 nm ($\mu_a = 0.033 \pm 0.005$ mm^{-1}, $\mu_s' = 1.94 \pm 0.11$ mm^{-1}). Unfortunately, the authors did not indicate the anatomic location where the cartilage was extracted. Descalle et al. harvested cartilage from porcine shoulder and foot joint and measured the diffuse reflectance, absorption, and reduced scattering coefficients of ligament and cartilage at 351 nm, 365 nm, and in the visible range (440–800 nm) [38]. The values of optical properties by Descalle et al. had similar tendencies with increasing wavelength.

The accuracy of the inverse adding-doubling method varies with the reflectance and transmittance of the sample [30]. For calculation of the absorption coefficient, the error is greatest when the total transmittance is highest [30]. On the other hand, error for the reduced scattering coefficient is greatest when little light is reflected by the sample [30]. Measurement of thickness and variation in thickness with water content is a major source of error. Additional sources of error are the loss of light from the edge of the sample and the problem of interference caused by the glass slides [39]. The first error manifests itself in higher calculated absorption values and may be reduced if a relatively large sample size compared with the beam diameter is used. For the latter error, use of wedge-shaped slides instead of glass slides will reduce this problem [39].

Various values for the refractive index of cartilage (i.e., $n = 1.40, 1.45, 1.50$) were used as an input parameter in the inverse adding-doubling computer program. The computed absorption coefficients decreased by approximately 2%, and the reduced scattering coefficients increased by approximately 2% with increasing refractive index. Although these variations were observed over the whole spectral range, the values were within the error of calculated values in Figure 4. The conclusion is that refractive index does not influence computed values of absorption and reduced scattering coefficients substantially.

A considerable variation was observed in thermal properties of cartilage (Table 1). The *t*-test results show that the thermal conductivity increased with higher temperature, and the thermal diffusivity values have no dependence on temperature. Observed variation may be due to measurement error, biological variability, or both. Although the former can be reduced by increased sample numbers, biological variability likely limits its accuracy of these measurements.

Values of thermal conductivity (k) and diffusivity (α) in cartilage were compared with other tissues such as a human rib at 37°C (k = 3.73–4.96 mW/cm°C), human cardiac muscle at 37°C (k = 4.92–5.62 mW/cm°C, $\alpha = 1.47 \times 10^{-3}$ cm^2/sec), and porcine skeletal muscle at 30–48°C (k = 4.3–5.1 mW/cm°C, $\alpha = 1.022 \times 10^{-3}$ cm^2/sec) [40]. These variations are likely caused by different structural compositions of the tissues.

A limitation of invasive thermal property measurement is the thermal probe insertion technique. When measuring cartilage thermal properties, we sought to minimize the gap between the inner surface of the cartilage cavity and the thermistor probe. Although the cavity is relatively smaller than the diameter of a probe and the probe fits snugly in the cartilage sample, errors introduced by the gap cannot be entirely eliminated. When micro air pockets are present in the gap, a thermal probe exchanges heat by conduction and radiation through air. The greater the air gap that is present at the inner surface of a cartilage cavity, the larger the error that will propagate in the measurement of thermal conductivity and diffusivity. Consequently, because the

conductivity and diffusivity of air in cartilage is low, we expect this artifact will give reduced thermal conductivity and diffusivity values. To reduce this error, the thermal probe insertion technique should be improved. One possibility to reduce the micro air gap between a thermal probe and the inner cavity of a cartilage sample is to place a viscous gel in the cavity before inserting a thermal probe. Another possibility is to manufacture a mechanically enhanced thermal probe so that the tip of the sensor can resist the stiffness of cartilage and interface better with the tissue surface in the cavity.

Another consideration for measurement of the thermal properties of cartilage is the sample mass change during the experiment. For measurements at 37 and 50°C, each sample mass was measured before and after the experiment. The sample mass after the experiment was reduced approximately 4.5% compared with the mass before the experiment. If all mass loss is due to water, the expected error in thermal properties for a 4.5% reduction in water content is 4.1% [1]. Therefore, we expect that the true thermal properties by using the invasive probe probably are approximately 4% higher than what was measured due to the loss of water. The mass reduction may originate in dehydration of the cartilage sample during measurement. To investigate the effect of water loss on the thermal conductivity and diffusivity values, accurate measurement of cartilage sample mass should be performed at each temperature.

Knowledge of the values of the thermal conductivity and diffusivity at different temperatures is significant to quantify heat transfer in cartilage during laser irradiation. When cartilage is heated under laser irradiation during reshaping, a phase transition occurs near 65°C [15]. Therefore, measurement of the thermal conductivity and diffusivity at additional temperatures should be performed (e.g., 62 and 75°C).

Inasmuch as the thermal controller system is designed to operate at 37°C, it is less accurate at other temperatures, particularly higher than 50°C and lower than 20°C. This limitation of the system is a result of design features and ambient noise in temperature measurements. The uncertainty of the measurement technique is approximately 2% for the temperatures less than 50°C and 5% for higher temperatures. In the future, the effect of water loss during higher temperature experiments should be considered and effect on measured thermal properties of cartilage should be investigated.

For the thermal diffusivity of cartilage obtained from infrared imaging radiometry, spatial resolution has been restricted by practical considerations. Our measurements indicate that IR imaging radiometry gives a value of thermal diffusivity consistent with the probe data. Although uncertainty for this measurement was relatively high, it can be reduced by modifying the current setup. First, the excitation laser beam diameter should be optimized with respect to characteristic thermal diffusion length, which is estimated from preliminary measurements. Second, improved spatial resolution of the IR-FPA camera may provide higher accuracy in measurements of thermal diffusivity. Infrared imaging radiometry has an advantage in that no contact with the specimen is required and may give more accurate results with greater computational economy.

REFERENCES

1. Welch AJ, van Gemert MJC. Optical-thermal response of laser-irradiated tissue. New York: Plenum Press; 1995.
2. Wong BJF, Milner TE, Kim HH, Nelson JS, Sobol EN. Stress relaxation of porcine septal cartilage during Nd:YAG (λ = μm) laser irradiation: mechanical, optical, and thermal response. J Biomed Opt 1998;3:409–414.
3. Wong BJF, Milner TE, Kim HK, Telenkov S, Chew C, Kuo T, Smithies DJ, Sobol EN, Nelson JS. Critical temperature transitions in laser mediated cartilage reshaping. Proc SPIE 1998;3425:161–172.
4. Wong BJF, Milner TE, Anvari B, Sviridov A, Omel'chenko A, Bagratashvili V, Sobol EN, Nelson JS. Thermo-optical response of cartilage during feedback controlled laser-assisted reshaping. Proc SPIE 1997; 2970:380–391.
5. Wong BJF, Milner TE, Anvari B, Sviridov A, Omel'chenko A, Bagratashvili V, Sobol EN, Nelson JS. Measurement of radiometric surface temperature and integrated backscattered light intensity during feedback controlled laser-assisted cartilage reshaping. Lasers Med Sci 1998;13:66–72.
6. Sobol EN, Bagratashvili V, Omel'chenko A, Sviridov A, Helidonis E, Kawalos G, Christodoulou P, Naoumidi I, Velegrakis G, Ovchinnikov Y, Shechter A. Laser shaping of cartilage. Proc SPIE 1994;2128:43–49.
7. Sobol EN, Bagratashvili V, Sviridov A, Omel'chenko A, Kitai M, Jones N, Zenger V, Nasedkin A, Isaev M, Shechter A. Study of cartilage reshaping with holmium laser. Proc SPIE 1996;2623:544–547.
8. Sobol EN, Bagratashvili V, Sviridov A, Omel'chenko A, Ovchinnikov Y, Svistushkin VS, Shechter A, Jones N, Howdle S, Helidonis E. Phenomenon of cartilage shaping using moderate heating and its applications in otorhinolaryngology. Proc SPIE 1996;2623:548–552.
9. Sobol EN, Sviridov A, Bagratashvili V, Omel'chenko A, Ovchinnikov Y, Shechter A, Downes J, Howdle S, Jones

N, Lowe J. Stress relaxation and cartilage shaping under laser radiation. Proc SPIE 1996;2681:358–363.
10. Sobol EN, Kitai M, Jones N, Sviridov A, Milner TE, Wong BJF. Theoretical modeling of heating and structure alterations in cartilage under laser radiation with regard of water evaporation and diffusion dominance. Proc SPIE 1998;3254:54–63.
11. Fischer R, Krebs R, Scharf HP. Cell vitality in cartilage tissue culture following eximer laser radiation: an in vitro examination. Lasers Surg Med 1993;13:629–637.
12. Freedland Y. Use of eximer laser in fibrocartilaginous excision from adjacent bony stroma: a preliminary investigation. J Foot Surg 1988;27:303–305.
13. Herman JH, Khosla RC. In vitro effects of Nd:YAG laser radiation on cartilage metabolism. J Rheumatol 1988;15: 1818–1826.
14. Pullin JG, Collier MA, Das P, Smith RL, DeBault LE, Johnson LL, Walls RC. Effects of holmium:YAG laser energy on cartilage metabolism, healing, and biochemical properties of lesional and perilesional tissue in a weight-bearing model. Arthroscopy 1996;12:15–25.
15. Sobol EN. Phase transformations and ablation in laser-treated solids. New York: John Wiley & Sons; 1995. p 316–322.
16. Ebert DW, Roberts C, Farrar SK, Johnston WM, Litsky AS, Bertone AL. Articular cartilage optical properties in the spectral range 300–850 nm. J Biomed Opt 1998;3: 326–333.
17. Woo LY, Buckwalter JA. Injury and repair of the musculoskeletal soft tissues. Park Ridge, IL: American Academy of Orthopaedic Surgeons; 1988.
18. Caplan AI. Cartilage. Sci Am J 1984;251:84–94.
19. Gray H. Gray's anatomy. New York: Gramercy Books; 1977.
20. Bowman HF, Cravalho EG, Woods M. Theory, measurement, and application of thermal properties of biomaterials. Annu Rev Biophys Bioeng 1975;4:43–80.
21. Chato JC. A method for the measurement of the thermal properties of biological materials. Thermal Problems in Biotechnology: winter annual meeting of the American Society of Mechanical Engineers. New York: Am Soc of Mech Eng. 1968; LCN068-58741:16–25.
22. Valvano JW, Cochran JR, Diller KR. Thermal conductivity and diffusivity of biomaterials measured with self-heated thermistors. International Journal of Thermophysics 1985;6:301–310.
23. Valvano JW, Chitsabesan B. Thermal conductivity and diffusivity of arterial wall and atherosclerotic plaque. Lasers Life Sci 1987;1:237–247.
24. Yuan DY, Valvano JW, Anderson GT. Measurement of thermal conductivity, thermal diffusivity, and perfusion. 30th Annual Rocky Mountain Bioengineering Symposium, San Antonio, TX. 1993.
25. Kirkland RW. In vivo thermal conductivity values for bovine and caprine osseous tissue. 20th Annual Conference on Engineering in Medicine and Biology, Boston, MA. 1967.
26. Bishnoi P. PC based multichannel thermal probe controller system. Thesis. The University of Texas at Austin; 1993.
27. Milner TE, Goodman DM, Tanenbaum BS, Anvari B, Nelson JS. Noncontact determination of thermal diffusivity in biomaterials using infrared imaging radiometry. J Biomed Opt 1996;1:92–97.
28. Wang XJ, Milner TE, Chang MC, Nelson JS. Group refractive index measurement of dry and hydrated type I collagen films using optical low-coherence reflectometry. J Biomed Opt 1996;1:212–216.
29. Thermometrics, Inc. Thermistors: thermocouples pressure sensors. Thermistor Catalog. Thermometrics, Inc. 1988; 183.
30. Prahl SA, van Gemert MJC, Welch AJ. Determining the optical properties of turbid media by using the adding-doubling method. Appl Opt 1993;32:559–568.
31. Hale GM, Querry MR. Optical constants of water in the 200-nm to 200-μm wavelength region. Appl Opt 1973;12: 555–563.
32. Curcio JA, Petty CC. The near infrared absorption spectrum of liquid water. J Opt Soc Am 1951;41:302–304.
33. Moore DS, McCabe GP. Introduction to the practice of statistics. New York: WH Freeman & Company; 1989.
34. Klier K. Absorption and scattering in plane parallel turbid media. J Opt Soc Am 1972;62:882–885.
35. van Gemert MJC, Star WM. Relations between the Kubelka-Munk and the transport equation models for anisotropic scattering. Laser Life Sci 1987;1:287–298.
36. Raunest J, Schwarzmaier HJ. Optical properties of human articular tissue as implication for a selective laser application in arthroscopic surgery. Lasers Surg Med 1995;16:253–261.
37. Beek JF, Blokland P, Posthnumus P, Aalders M, Pickering JW, Sterenborg HJCM, van Gemert MJC. In vitro double-integrating-sphere optical properties of tissues between 630 and 1064 nm. Phys Med Biol 1997;42:2244–2261.
38. Descalle M-A, Jacques SL, Prahl SA, Laing TJ, Martin WR. Measurements of ligament and cartilage optical properties at 351 nm, 365 nm and in the visible range (440–800 nm). Proc SPIE 1998;3195:280–286.
39. Pickering JW, Prahl SA, van Wieringen NV, Beek JF, Sterenborg H, van Germert MJC. Double-integrating-sphere system for measuring the optical properties of tissue. Appl Opt 1993;32:399–410.
40. Duck FA. Physical properties of tissue: a comprehensive reference book. London: Academic Press; 1990. p 9–65.